



AC conductivity and dielectric characteristics of PVA/PVP nanocomposite filled with MWCNTs

E. M. Abdelrazek^{1,2} · A. M. Abdelghany³ · A. E. Tarabiah⁴ · H. M. Zidan⁵

Received: 2 March 2019 / Accepted: 24 July 2019 / Published online: 27 July 2019
© Springer Science+Business Media, LLC, part of Springer Nature 2019

Abstract

AC electrical conductivity σ_{ac} of PVA/PVP blend filled with MWCNTs was studied using impedance spectroscopy over a wide frequency range of 10^{-1} to 10^7 Hz at different fixed temperatures. It was observed that the frequency-dependent nature of the ac electrical conductivity followed the Jonscher's law and the increasing of MWCNTs content in the polymeric matrix leads to form a percolating network through the composite. On the contrary, a conductivity reduction is observed for the composition of 5 wt% of MWCNTs, which may be ascribed to the aggregation occurred in nanotubes and consequently loss of percolation. The CBH model has been suggested to agree with the conduction mechanism of σ_{ac} for the present system. Also, the maximum barrier height over which the electrons hop decreases with increasing temperature. Impedance data were studied in terms of electrical modulus formalisms M^* and impedance formalisms Z^* . The relation between real and imaginary parts of complex impedance shows an inclined spike at low frequency and a semicircular arc at high frequency with radius decrease with increasing the temperature and could be best fitted to two equivalent circuit models. The analysis of M'' and Z'' spectra indicates that the distribution of relaxation times is independent of the temperature. The non-coincidence of peaks corresponding to M'' and Z'' indicates the deviation of non-Deby relaxation and short-range movement of charge carriers. The activation energy values, which are determined from the bulk conductivity and electric modulus, are very close.

1 Introduction

Elastic and lightweight polymeric dielectric/conducting materials are becoming a necessity in microelectronic devices these years. The electrical properties of the polymers are generally known to be improved by filling them with a lot of conducting types of filler [1]. The filling of conductive fillers such as metallic particulates/fibers and

carbon black to the polymer matrices, above a percolation threshold, increases the conductivity abruptly. Percolation appears because of the buildup of three-dimensional conductive paths in the polymeric matrix [2, 3]. Functional studying of such polymeric composites required the continuous practice to allow enhancement of their electrical conductivity at small filler concentrations. Consequently, mechanical features of pure polymers could be kept without suffering from fragile behavior. Furthermore, the addition of fillers with a high aspect ratio exhibit percolation at a very low filler content [4].

Carbon nanotubes (CNTs) have been extensively studied because of their outstanding physical, mechanical and electronic properties. Electrical percolation of CNTs/polymer composites was recently studied by Bauhofer and Kovacs [5]. They found that the percolation threshold depends on different parameters such as synthesis method, CNTs type, dimensionality and polymer matrix type.

Polyvinyl alcohol (PVA) is a polar polymer with hydroxyl groups linked to methane carbons with a carbon chain backbone. PVA composites formation is because of the OH groups, which can be shared in hydrogen bonding. PVA has a good charge storage capacity, high dielectric strength,

✉ A. M. Abdelghany
a.m_abdelghany@yahoo.com

¹ Physics Department, Faculty of Science at Al-Ula, Taibah University, Medina, Saudi Arabia

² Physics Department, Faculty of Science, Mansoura University, Mansoura 35516, Egypt

³ Physics Division, Spectroscopy Department, National Research Center, 33 Elbehouth St, Dokki, Cairo 12311, Egypt

⁴ Dental Biomaterials Department, Faculty of Oral & Dental Medicine, Delta University for Science & Technology, Gamasa, Egypt

⁵ Physics Department, Faculty of Science, Damietta University, Damietta 34517, Egypt

and filling dependent optical and electrical properties. The improvement of the electric, dielectric, and optical features of the host matrix was observed by filling the PVA with chalcogenide semiconductors and metal oxide semiconductors. This has led to making the PVA polymer a potential candidate in electronics and optoelectronics industry [6].

Polyvinylpyrrolidone (PVP) has excellent physiological compatibility, good film forming, good environmental stability, and moderate electrical conductivity. Both of the PVA and PVP are miscible and soluble in water in all proportions [7]. PVA/PVP blend is used in medicine as a skin dressing component and in the electrochemical area as a polyelectrolyte or membrane [7].

Structural investigations combined with optical measurements were previously investigated [8] by the same research group concluding the intermolecular interaction between polymeric matrix and filler with the formation of polarons and/or bipolarons in the polymeric matrices. They also indicated that the refractive index follow the anomalous dispersion within the wavelength range (190–866) and normal dispersion in the wavelength range (866–2500) using single oscillator model. Critical variations was also observed on single oscillator energy E_o and the dispersion energy E_d at the 0.5 MWCNT's concentration.

The recent study examines developing elastic and light-weight polymer nanocomposites with enhanced electrical properties prepared by solution casting technique for electronic applications. In this work, PVA/PVP blend has been selected as host polymer matrix with multi-walled carbon nanotubes (MWCNTs) as a conducting filler. The complex impedance spectroscopy and AC electrical conductivity can be used to study the effect of MWCNTs on the electrical and dielectric properties of PVA/PVP blend filled with different MWCNTs contents. The behavior of the samples studied was analyzed by the impedance data as a function of frequency (10^{-1} to 10^7 Hz) at different temperatures (303 to 343 K). In addition, the conduction mechanism was also studied.

2 Experimental work

In the present work, PVP (supplied by SISCO Research Laboratory Pvt. Ltd. Mumbai, India—M.W. 40000) and PVA (supplied by S.D. Fine-Chem Ltd. Mumbai, India—M.W. 14,000) were provided. These polymers were used as a blend matrix material for MWCNTs filling developed by chemical vapor deposition (CVD).

Nanothinx functionalized MWCNTs (NTX10) were added to distilled water and sonicated for 15 min. Equal quantities of PVP and PVA were blended with this solution and stirred at 70 °C until a suitable viscous solution had formed. To prepare the filled polymeric films, this viscous solution is then transferred to Petri dishes and dried in an

oven for 2 days at 60 °C. During drying, the films were detached from Petri dishes and stored in vacuum desiccators until they are used. The amounts of MWCNTs inside the PVA/PVP mixture are 0, 1, 3, 5 wt%. The samples thickness was between 0.005 and 0.01 cm.

AC electrical studies were done in a frequency range of 10^{-1} to 10^7 Hz, by using Novocontrol Technologies Broadband Dielectric Spectroscopy. The measured temperature range was from 303 to 343 K. All the measurements were done in an evacuated system to eliminate the effect of moisture.

3 Result and discussion

3.1 Conductivity studies

The conductivity frequency dependence is a popular response of amorphous polymers because of the large increase in the mobility of charge carriers inside the polymeric matrix. The frequency variation studies were done to realize the electrical homogeneity of the material by characterizing the nature of electrical conduction and relaxation mechanism. Using impedance spectroscopy, a sinusoidal voltage of different frequencies in AC conductivity measurements was applied across the sample. If f is the frequency of the signal applied, then the AC conductivity σ_{ac} can be calculated by the following relation:

$$\sigma_{ac} = 2\pi f \epsilon' \epsilon_0 \tan \delta \quad (1)$$

where ϵ_0 and ϵ' are the dielectric constant of the free space and the material respectively and $\tan \delta$ is the loss tangent or dissipation factor.

Figure 1 represents logarithmic plots of the change in AC conductivity versus frequency for the studied samples at room temperature. It is appearing that the σ_{ac} increases with increasing the MWCNTs and there is an abrupt increase at 1 wt% MWCNTs suggesting a percolation behavior. The low value of the percolation threshold suggested uniform dispersion of MWCNTs in the polymeric matrix and interaction takes place. This interaction gives rise to an effective conductive pathway in the polymer matrix. This finding is confirmed by previous reports [9]. They studied the electrical behavior of PVA/MWCNTs composites. They found the percolation phenomena in these samples and the percolation threshold is between 0.65 and 0.70 wt% [9]. Generally, the conductivity of the present system was observed to increase with the MWCNTs content increase up to 3 wt%. This can be ascribed to the increase in the number of conductive paths formed by dispersed MWCNTs in the polymeric matrix. It is known that the electrical conductivity of such composites depends on the filler type, shape, size, and dispersion in the composites [9, 10]. In addition, the increase in conductivity

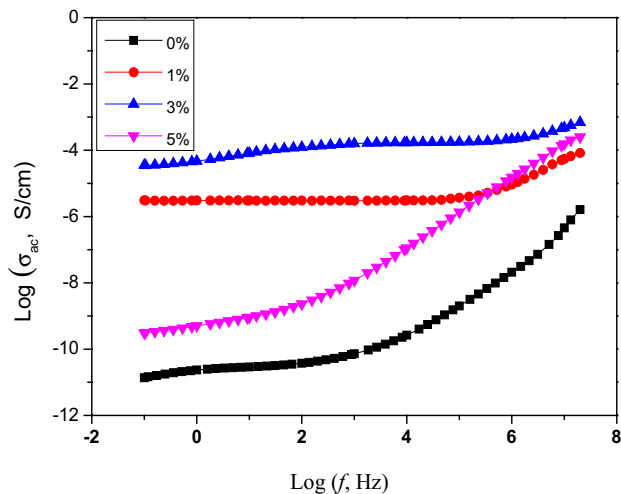


Fig. 1 The change of $\text{Log}(\sigma_{ac})$ as a function of $\text{Log}(F)$ for PVA/PVP blend filled with different MWCNTs content at room temperature

may be due to the increase in the amorphous nature of the polymer composite, which decreases the energy barrier and thus facilitates the ion transport. However, a conductivity reduction is observed for the composition with 5 wt% of MWCNTs. This may be due to the aggregation occurred in nanotubes and consequently loss of percolation [11]. Ion aggregation reduces the number of mobile charge carriers and thus the conductivity [12, 13].

It can be seen that the electrical conductivity σ_{ac} increases with the frequency. In addition, composites with filler loading higher than percolation threshold exhibit two regions. The first region has the conductivity nearly constant in the low-frequency range (as plateau region), and the second region (dispersion region) has the conductivity dependent on the frequency at the high-frequency range, obeying the power law.

The plateau region is associated with the DC conductivity σ_{dc} and ascribed to the bulk conductivity of the sample occurring due to the displacement of charge carriers [10]. The σ_{dc} value was calculated by extrapolating the plateau regions to the $\text{Log} \sigma_{ac}$ axis and measuring the intersections at zero frequency. In the high-frequency range (dispersion region), the conductivity raises linearly with the frequency. The mobility of charge carriers is higher in the high-frequency range [14]. As the MWCNTs content increase, it has been found that the conductivity increases and the high-frequency dispersion is shifted towards the highest frequency side.

Zhang et al. [9] explained the frequency dependence of σ_{ac} in terms of the polarization effects by establishing an analogy between the composite samples and a resistor–capacitor equivalent circuit, in which there is capacitance between the conductive filler clusters. According to

their reports, the conductivity for composites with MWCNTs higher than the percolation threshold is generally determined by the numerous paths of the percolating clusters rather than the capacitors.

Thus the composites conductivity does not change with the variation of the frequencies up to a certain frequency, above which the contribution of the capacitors becomes dominant, and so a plateau is observed in AC conductivity–frequency diagram below this frequency. Moreover, in the composite whose MWCNTs content is near the percolation threshold, there are only a small number of percolating cluster paths, so that the AC conductivity contribution of the capacitors between the clusters becomes important. As the frequency increases, the current flowing through each capacitor increases, which improves the conductivity of the composites.

Figure 2 shows the change in $\text{Log}(\sigma_{ac})$ versus frequency at different temperatures for different contents of MWCNTs in the present system. It is found that σ_{ac} raises with the increase in temperature like the behavior regarded in a lot of polymers and semiconductors [14]. Where, the increase in the temperature increases the mobility of charge carriers in the composite and also, increases the number of transit sites [15]. This enables the charge carrier to move from one transit site to another without gaining much energy (more charge carriers will overcome the potential barrier and participate in the electrical conduction). In general, the frequency at which the dispersion occurs is known as the hopping frequency, which shifts toward higher frequency region as temperature increase (as shown in Fig. 2). This feature suggests the existence of a hopping type mechanism for electrical conduction in the material that is governed by the Jonscher’s power law [15].

$$\sigma_{ac}(\omega) = \sigma_{dc} + A\omega^s \quad (2)$$

where $\omega = 2\pi f$ is the angular frequency, σ_{dc} is the DC conductivity (i.e., independent of frequency at $\omega \cong 0$), A is a temperature-dependent constant and determines the strength of polarizability, and s is an exponent dependent on both temperature and frequency with value $0 \leq s \leq 1$. This is a typical manner for a lot of materials and is called by Jonscher ‘universal dynamic response’ (UDR).

The exponent “s” indicates the degree of interaction between the lattice and mobile ions, and its change with the temperature and frequency represents the type of conduction mechanism that exists in the material. Different theoretical models, like quantum mechanical tunneling (QMT), correlated barrier hopping (CBH), non-overlapping small polaron tunneling (SPT) and overlapping large polaron tunneling (OLPT) are used to identify the conduction mechanism of the AC conductivity [16]. The QMT model is based on phonon-assisted electron tunneling and predicts a little increase of s with increasing temperature or independent of

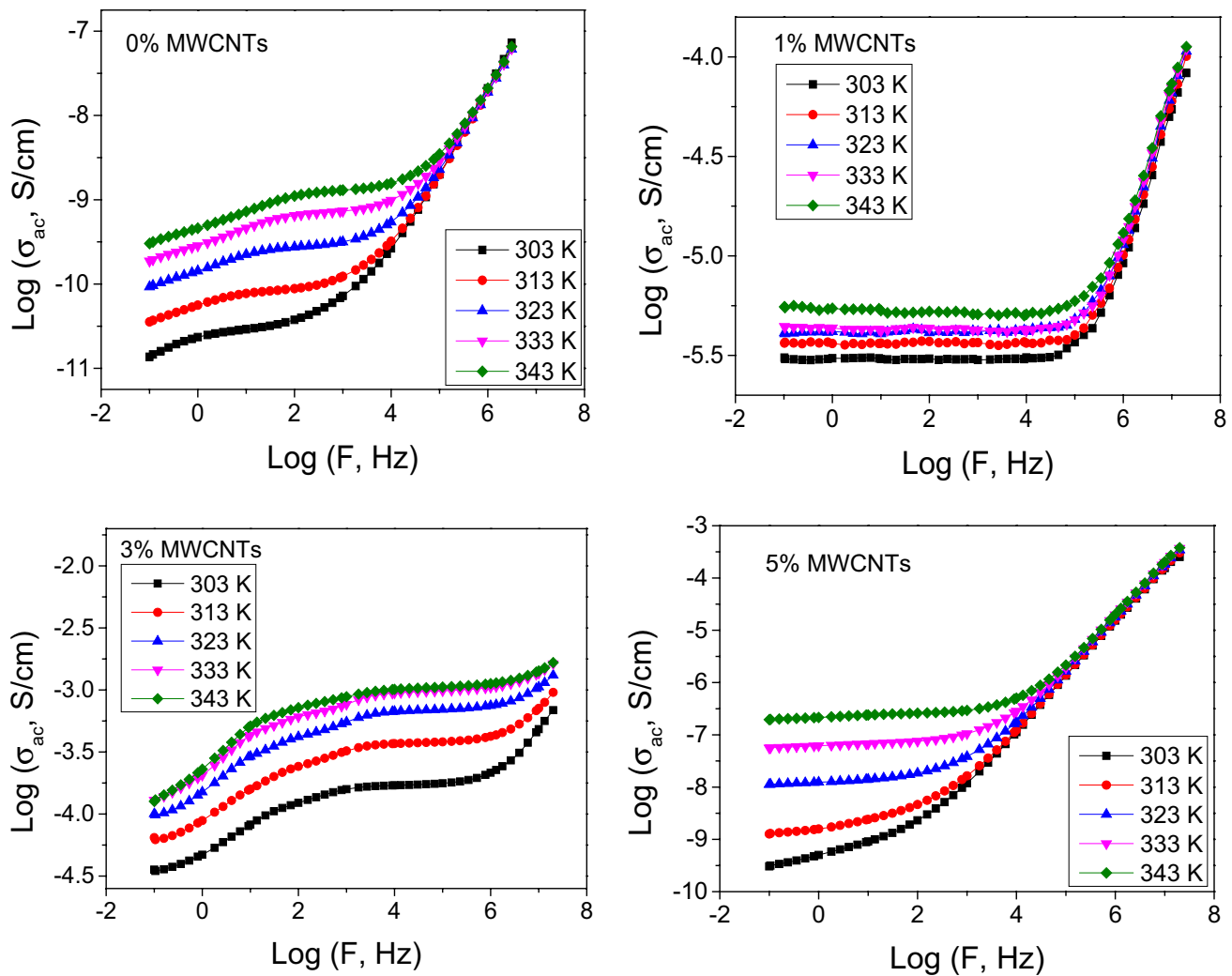


Fig. 2 The change of $\text{Log}(\sigma_{ac})$ as a function of $\text{Log}(F)$ for PVA/PVP blend filled with different MWCNTs content at different temperatures

temperature, with value nearly equal/around 0.8. The CBH model assumes that the charge carriers hop between two sites above the Coulomb barrier, which separates them, and that the exponent s values decrease with increasing temperature. The SPT model predicts a monotonous increase of s with temperature increase, while the OLPT model predicts that s will decrease with temperature increase up to a certain temperature and then increases with further increase in temperature.

The value of s at a certain temperature can be obtained from the slope of the linear behavior in the high-frequency dispersion region in Fig. 2. Figure 3 displays the behavior of the frequency exponent s for the present system with temperature in the temperature range 303–343 K. It is appearing that the values of s for all samples decrease with increasing temperature. This supports that the CBH model has been suggested to correlate the conduction mechanism of σ_{ac} for the present samples.

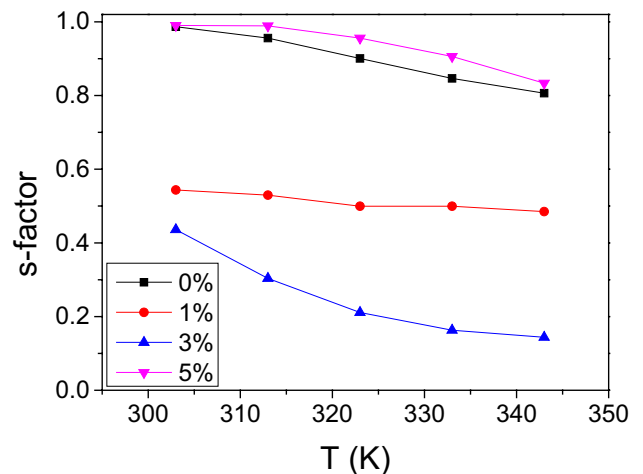


Fig. 3 Temperature dependence of (s -factor) for PVA/PVP blend filled with different MWCNTs content

In this model, the temperature dependence of frequency exponent s is given by:

$$s = 1 - \frac{6K_B T}{W_M - K_B T \ln\left(\frac{1}{\omega \tau_0}\right)} \tag{3}$$

where τ_0 is the characteristic relaxation time that is in the order of an atom vibrational period ($\approx 10^{-13}$ s), K_B is Boltzmann’s constant, and W_M is the maximum barrier height at infinite separation (the energy needed to make the electron moving from a site to infinity) i.e. the binding energy of the charge carriers at their localized sites. For an approximation of this relation, the exponent s becomes:

$$s = 1 - \frac{6K_B T}{W_M} \tag{4}$$

The average value of the binding energy W_M can be obtained from the slope of the plotting $(1 - s)$ vs. T . Figure 4 shows the change of W_M as a function of temperature for PVA/PVP blend filled with different contents of MWCNTs. It can be seen that W_M decreases with the temperature increase, which correlates to the decrease in the exponent s . Thus, the number of free charge carriers that can hop over the barrier is increased. This behavior confirms the increase of σ_{ac} with temperature [11].

The AC conductivity can be expressed in terms of hopping between localized states at the Fermi level and evaluated by [12]:

$$\sigma_{ac} = [N(E_F)]^2 T K_B e^2 \alpha^{-5} \omega \left[\ln\left(\frac{\nu_{ph}}{\omega}\right) \right]^4 \tag{5}$$

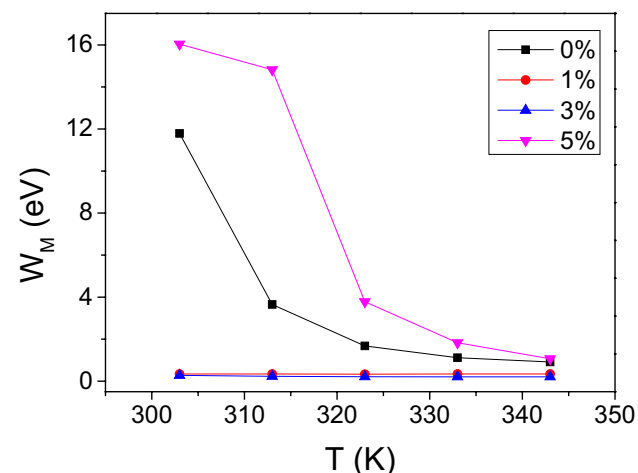


Fig. 4 Temperature dependence of W_M for PVA/PVP blend filled with different MWCNTs content

where ν_{ph} is the phonon frequency and α is the exponential decay parameter of localized states wave functions and $N(E_F)$ is the density of states at the Fermi level. The value of $N(E_F)$ can be obtained from Eq. (5) by substituting on the value of $\alpha^{-1} = 10 \text{ \AA}$ and $\nu_{ph} = 10^{12} \text{ s}^{-1}$ [13, 17]. Figure 5 shows the change of $N(E_F)$ with temperature for PVA/PVP blend filled with different contents of MWCNTs. It can be seen that the $N(E_F)$ values increases with increasing temperature for all filling levels of MWCNTs in the blend. This confirms the increase in the number of charge carriers contributing to the conduction process with filling level and temperature.

The variation of σ_{dc} with the reciprocal of temperature for the present system can be represented in Fig. 6. The linear

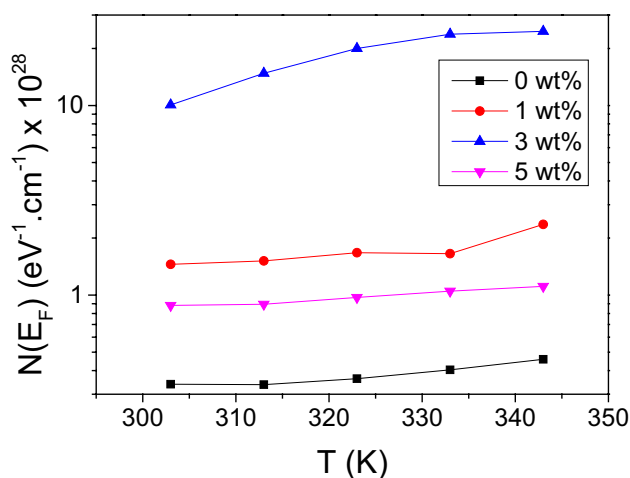


Fig. 5 Temperature dependence of $N(E_F)$ for PVA/PVP blend filled with different MWCNTs content at a selected frequency (100 kHz)

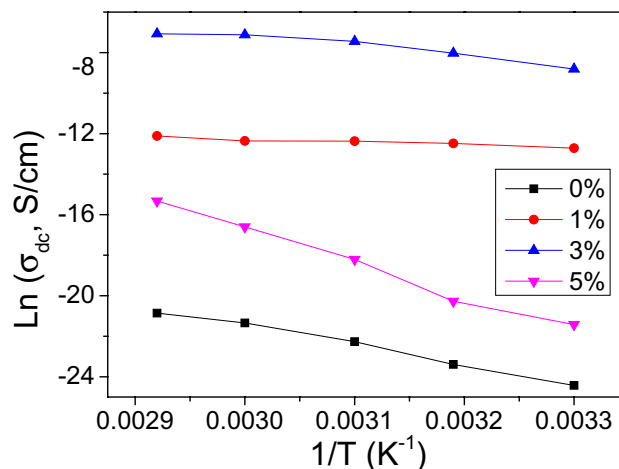


Fig. 6 The change of $\text{Ln}(\sigma_{dc})$ as a function of $1/T$ for the present system

behavior suggests a thermally activated process obeys the Arrhenius relation:

$$\sigma_{dc} = \sigma_0 \exp(-E_{dc}/K_B T) \tag{6}$$

where σ_0 is the pre-exponential factor, E_{dc} is the thermal activation energy for DC conductivity. The activation energy E_{dc} can be obtained from the slope of the plots and listed in Table 1.

Figure 7 shows the plots of $\text{Ln}(\sigma_{ac})$ versus $1/T$ at chosen frequencies. The values of the activation energy are calculated from the slope of the set lines and listed in Table 2. It is observed that the activation energy E_{ac} decreases with the increase in frequency, suggesting that the frequency of the

applied field improves the ionic jumps between localized states, further proving that the dominant mechanism is the hopping conduction. On the other hand, at high frequencies, the conductivity is dominated by the mobility of charge carriers over a short distance, which requires less energy than that required for mobility over a longer distance at low frequency [18].

3.2 Impedance studies (Z^*)

To Interpret the dielectric spectra, various formalisms such as complex impedance Z^* and complex electric modulus M^* have been explored [19]. The utilization of M^* formula is favorable when localized relaxation dominates to the capacitive and/or resistive analysis, but if the long-range conduction dominates, the Z^* formula is convenient. The complex impedance can be evaluated from [20]:

$$Z^* = Z' - iZ'' = \frac{1}{i\omega\epsilon_0\epsilon^*} \tag{7}$$

Table 1 The activation energy E_{dc} for the present system

| MWCNTs (wt%) | E_{dc} (eV) |
|--------------|---------------|
| 0 | 0.83 |
| 1 | 0.11 |
| 3 | 0.40 |
| 5 | 1.43 |

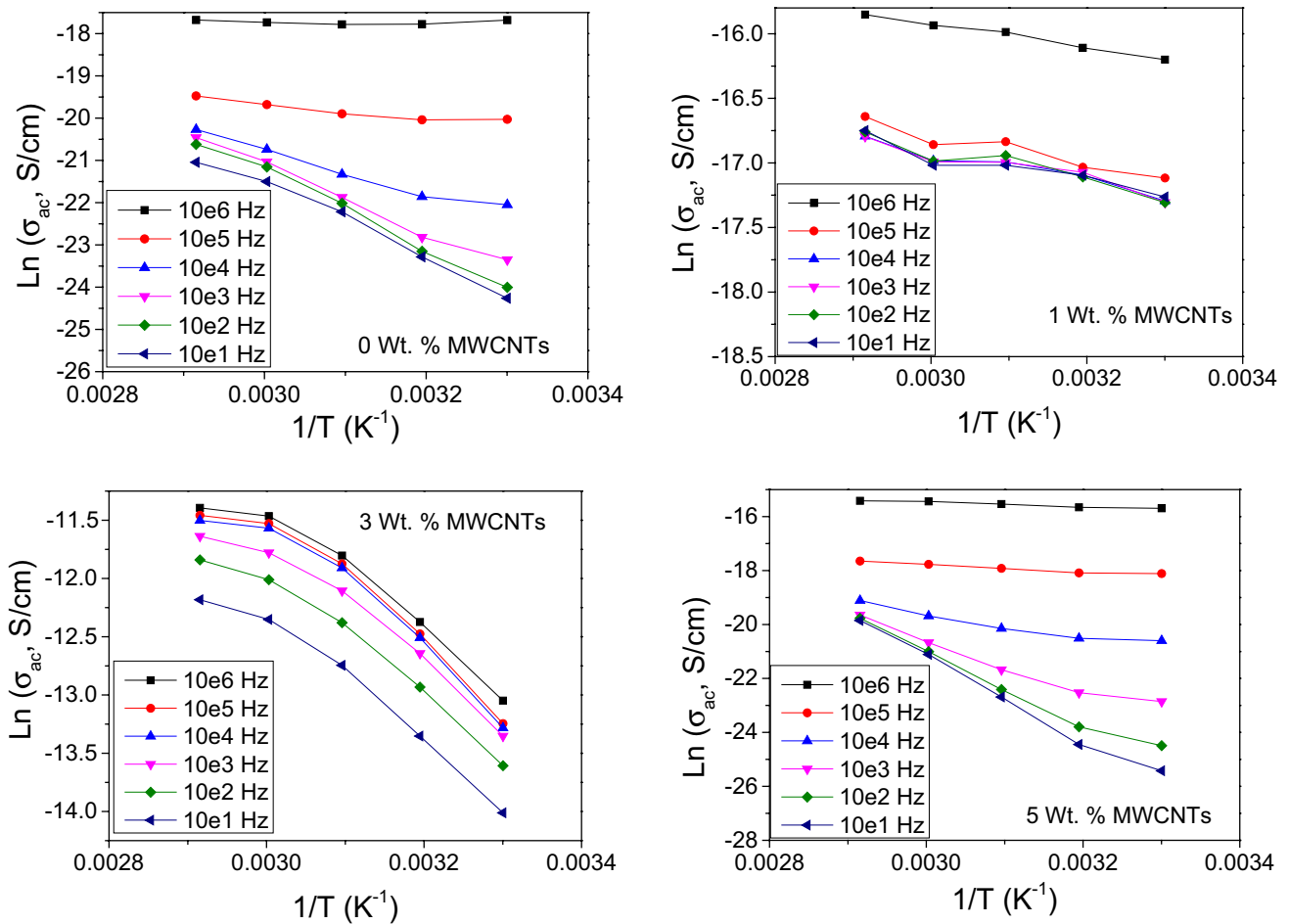


Fig. 7 The change of $\text{Ln}(\sigma_{ac})$ as a function of $1/T$ at selected frequencies for the present system

Table 2 The activation energy E_{ac} at different frequencies for the present system

| MWC-NTs (wt%) | Frequency (Hz) | E_{ac} (eV) |
|---------------|----------------|---------------|
| 0 | 10^6 | 0.002 |
| | 10^4 | 0.410 |
| | 10^2 | 0.786 |
| 1 | 10^6 | 0.078 |
| | 10^4 | 0.090 |
| | 10^2 | 0.109 |
| 3 | 10^6 | 0.381 |
| | 10^4 | 0.400 |
| | 10^2 | 0.401 |
| 5 | 10^6 | 0.068 |
| | 10^4 | 0.340 |
| | 10^2 | 1.090 |

Particularly, the direct separation of the bulk and bulk/electrode interface phenomena is allowed by using Z^* formalism [21].

Investigation of ionic conductivity of the polymeric material is done by impedance spectroscopy. The shape of impedance spectra gives the information on the electrode polarization and the kind of charge carriers electrons or ions. Figure 8 shows the Nyquist curves (Z'' vs. Z') of the investigated system at temperatures of 303 K and 343 K in the frequency range 10^{-1} – 10^7 Hz with the equivalent circuit elements. It has been found that the impedance plane plot i.e. Cole–Cole plots of the films consists of the inclined spike at low frequency and depressed semicircular arc at high frequency. The inclined spike and the semicircle together represent the characteristic behavior of ionic conducting materials [22]. The semicircle represents the parallel combination of bulk capacitance (because of the immobile polymer chains) and bulk resistance (because of ions migration). Therefore, the frequency of the present sample response can be indicated by a parallel combination of the circuit element R (resistance) and capacitance as an equivalent circuit.

The inclined spike refers to double layer capacitance formation at the electrode/electrolyte interface because of ions migration at low frequency. The capacitance values are in the range of PF, which indicate to the sample bulk response [23]. At each interface, the electrode double layer possesses an increase of impedance against ion transfer with decreasing frequency, which was represented by an inclined spike in the Nyquist plot of impedance spectra [24]. Moreover, the spike inclination at an angle lower than 90° to the real axis is because of the roughness of the electrode/electrolyte interface [25].

It is found that in the investigated temperature range the diameter of semicircles (represent the bulk resistance R_b) decrease with the temperature increase, showing the

presence of activated conduction mechanism [26]. Also, it is observed that the spike is elongated and the semicircle diameter is decreased with MWCNTs content increase. According to these results, when the filler content is increased, only the resistive component of composite prevails. The capacitive nature vanishes because of the random orientation of the dipoles in the polymer side chains [27]. The presence of the depressed semicircle, which its center below the real axis, imply that the relaxation process is non-Debye type. This deviation is because of the potential well for each site, through which the ion transport takes place, not being equal [28].

Modeling of impedance data can be usually represented by an equivalent circuit composed of resistant and capacitance to clarify the relation between microstructure and electrical properties. Using EIS software, the obtained impedance data was fitted with an equivalent circuit. This circuit composed of a parallel combination of resistance R_b and fractal capacity CPE_1 ($R_b \parallel CPE_1$) in series with fractal capacity CPE_2 as shown in the inset of Fig. 8. CPE refers to a constant phase element indicating the departure from ideal Debye type model. In this model R_b indicates to the bulk resistance, CPE_1 and CPE_2 are simple distributed elements that produce impedance having a constant phase angle in the complex plane. The impedance of the CPE is explained through the following relation.

$$Z_{CPE} = 1/Q(i\omega)^n \quad (8)$$

where Q is the numerical value of $1/|Z|$ at $\omega = 1 \text{ rad s}^{-1}$ and n is the phase of the elements and give the degree of deviation with respect to the pure capacitor. The CPE works like a pure resistor when $n=0$ and pure capacitor when $n=1$. The very good agreement between the data and the modeling results confirms that the selected equivalent circuit is a convenient choice.

The parameters corresponding to the equivalent circuit model are obtained from the fitting of the curves of Fig. 8 and are tabulated in Table 3. This table shows that the bulk capacitance values (Q_1) have values in the range of PF. Also the bulk resistance R_b was observed to decrease with temperature increase because of charge carriers mobility increase [29].

Figure 9 reflects the change of Z' with the frequency at various temperatures for PVA/PVP blend filled with 3 wt% MWCNTs (as a representative sample). It is observed that the values of Z' decrease gradually with increasing temperature and frequency, indicating the increase in the σ_{ac} [30]. On the other hand, the values of Z' become nearly zero at the high-frequency range and independent on temperature which could be because of the release of space charge at high temperatures [31].

Figure 10 reflects the change of Z'' with the frequency at various temperatures for PVA/PVP blend filled with 3

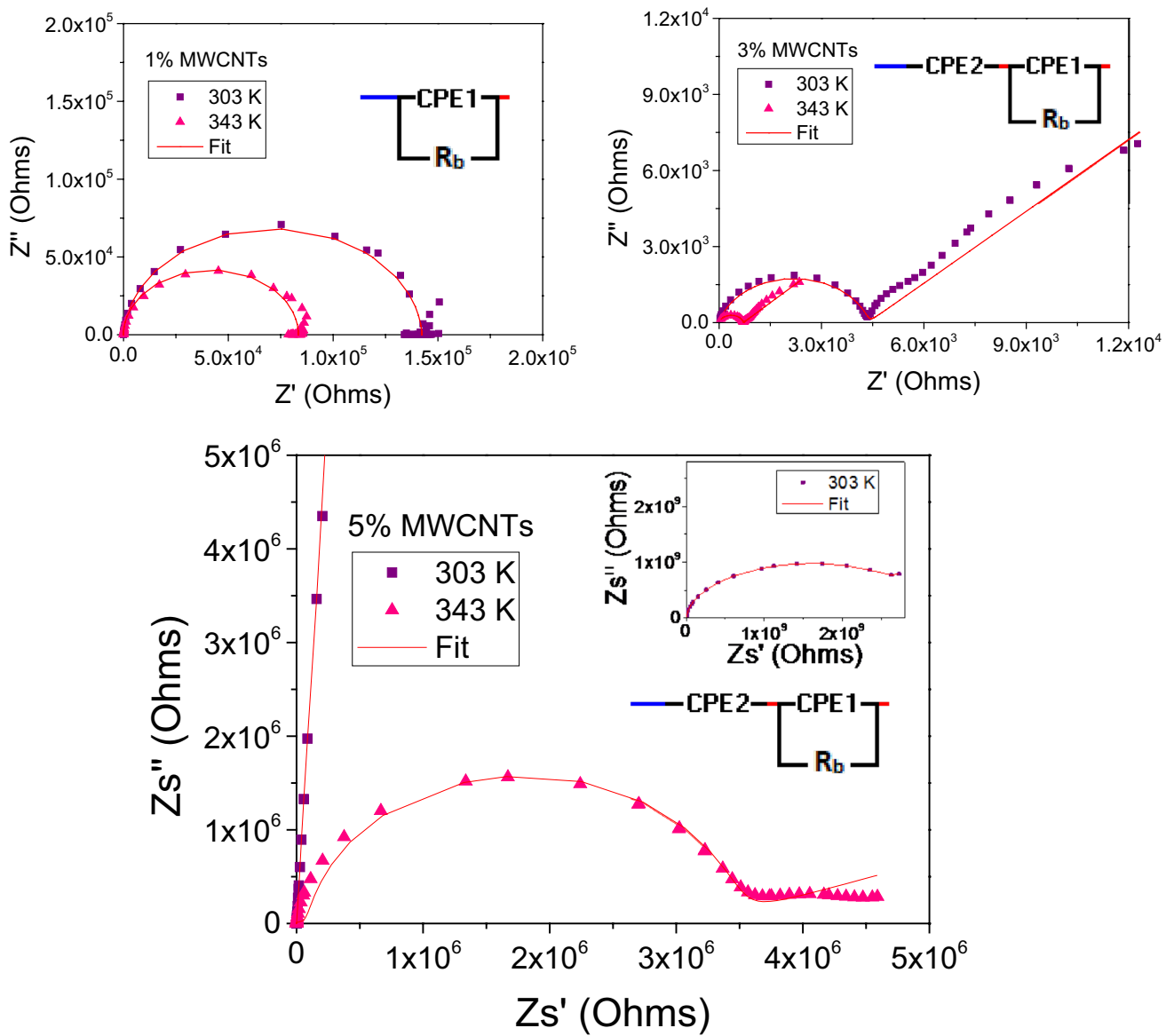


Fig. 8 Nyquist plots for PVA/PVP blend filled with different MWCNTs content at temperatures 303 K and 343 K (asterisks are the experimental points, and the solid line represents the result of fitting)

Table 3 Summarizing of fitting parameters corresponding to equivalent circuit model

| MWCNTs (wt%) | Temperature (K) | Fitting parameters | | | | |
|--------------|-----------------|--------------------|------------------------|-------|-----------------------|-------|
| | | $R_b(\Omega)$ | $Q_1(F)$ | n_1 | $Q_2(F)$ | n_2 |
| 1 | 303 | 1.42×10^5 | 7.19×10^{-11} | 0.97 | | |
| | 343 | 8.34×10^4 | 5.74×10^{-11} | 1 | | |
| 3 | 303 | 4.36×10^3 | 7.89×10^{-10} | 0.84 | 3.39×10^{-5} | 0.47 |
| | 343 | 6.82×10^2 | 2.81×10^{-10} | 0.91 | 2.38×10^{-4} | 0.41 |
| 5 | 303 | 1.90×10^9 | 1.27×10^{-10} | 0.87 | 1.22×10^{-9} | 0.89 |
| | 343 | 3.19×10^6 | 9.35×10^{-11} | 0.96 | 7.47×10^{-7} | 0.22 |

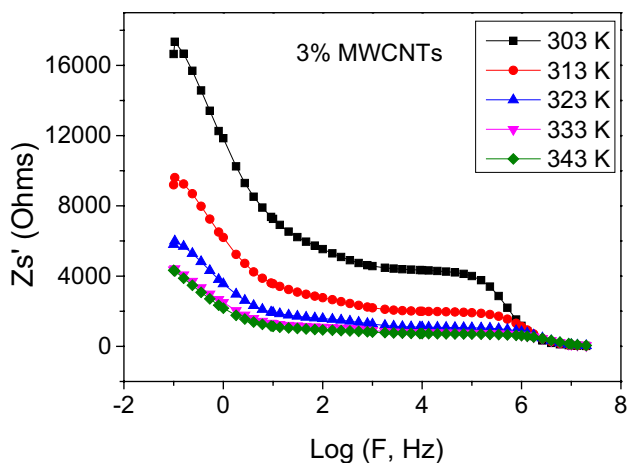


Fig. 9 The change of the real part Z' of complex impedance as a function of $\text{Log}(F)$ for PVA/PVP blend filled with 3 wt% of MWCNTs (as a representative sample) at different temperatures

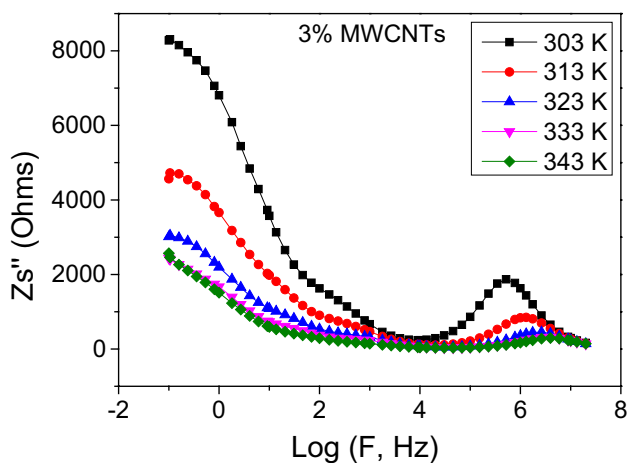


Fig. 10 The change of the imaginary part Z'' of complex impedance as a function of $\text{Log}(F)$ for PVA/PVP blend filled with 3 wt% of MWCNTs (as a representative sample) at different temperatures

wt% MWCNTs (as a representative sample). The spectra are characterized by a well-defined broad peak with significant asymmetry. As the temperature rises, Z'' peak maximum shifts to a higher frequency and the height of the peak decreases gradually. These findings imply a spread of relaxation time in the system [32]. Also, in the high-frequency region all the Z'' overlap. This behavior implies the accumulation of space charge polarization effect in the material at high temperature and low frequency [33].

3.3 Complex electric modulus (M^*)

The complex electric modulus M^* was utilized to study the conductivity relaxation phenomena. This formalism advantage is to remove the electrode effect [34]. And is favorable

to detect and distinguish the difference between the bulk effects and electrode polarization phenomenon [35]. The M^* can be evaluated from these equations:

$$M^* = M' - iM'' = 1/\epsilon^* = \frac{\epsilon' + i\epsilon''}{(\epsilon')^2 + (\epsilon'')^2} \tag{9}$$

$$M' = \epsilon' / (\epsilon'^2 + \epsilon''^2) \tag{10}$$

$$M'' = \epsilon'' / (\epsilon'^2 + \epsilon''^2) \tag{11}$$

where M' , M'' , ϵ' and ϵ'' are the real and imaginary parts of the electric modulus and dielectric constants, respectively.

Figures 11 and 12 display the change of M' and M'' with frequency for the present system. It is observed that the values of M' and M'' approach almost zero at low frequencies, where the charge carriers mobility is reduced due to missing of the restoring force governing it. Low values of M' and M'' indicate that the electrode effect has a negligible contribution of electrode polarization and thus can be ignored. The step-like transition relative to the frequency reach an asymptotic value and reflect that the nature of the samples is highly capacitive.

Figure 12 shows well defined broad peaks with significant asymmetry which gives an indication to the nature of the relaxation processes exist. The existence of relaxation peak in M'' curves means that the samples are probable ionic conductors [36]. As the temperature increased M'' peak shifts to a higher frequency and the height of the peak increased gradually, which mean conductivity relaxation indicating that the dielectric relaxation is thermally activated, where the charge carriers hopping is predominant [37]. Also, the peak shifting in the forward direction with temperature mean that the relaxation time decreases with temperature increase. The relaxation time is basically segmental motion and dipole orientation facilitated by the temperature increase. The maximum value of the peak decreases for the filled films as compared to the pure blend suggesting that the MWCNTs contributes to the relaxation process. The asymmetric nature of the curve and the broad M'' peaks can be explained as being the result of the distribution of relaxation time and deviation from the ideal Debye type behavior [38].

Two relaxation regions are appeared below and above M''_{max} . The region of the left side of the peak (low frequency) can be related to the DC conductivity result from the continuous hopping process, in which the charge carriers are mobile over long distances. However, the region of the right side of the peak (high-frequency side) is related to the relaxation polarization process and show the range of frequencies where the ions are spatially restricted to their potential wells and the ions can only make short-range motion within the wells [39]. The right side of the peak related to the AC conductivity results from the reversible ion movement over limited space. Thus the peak frequency is

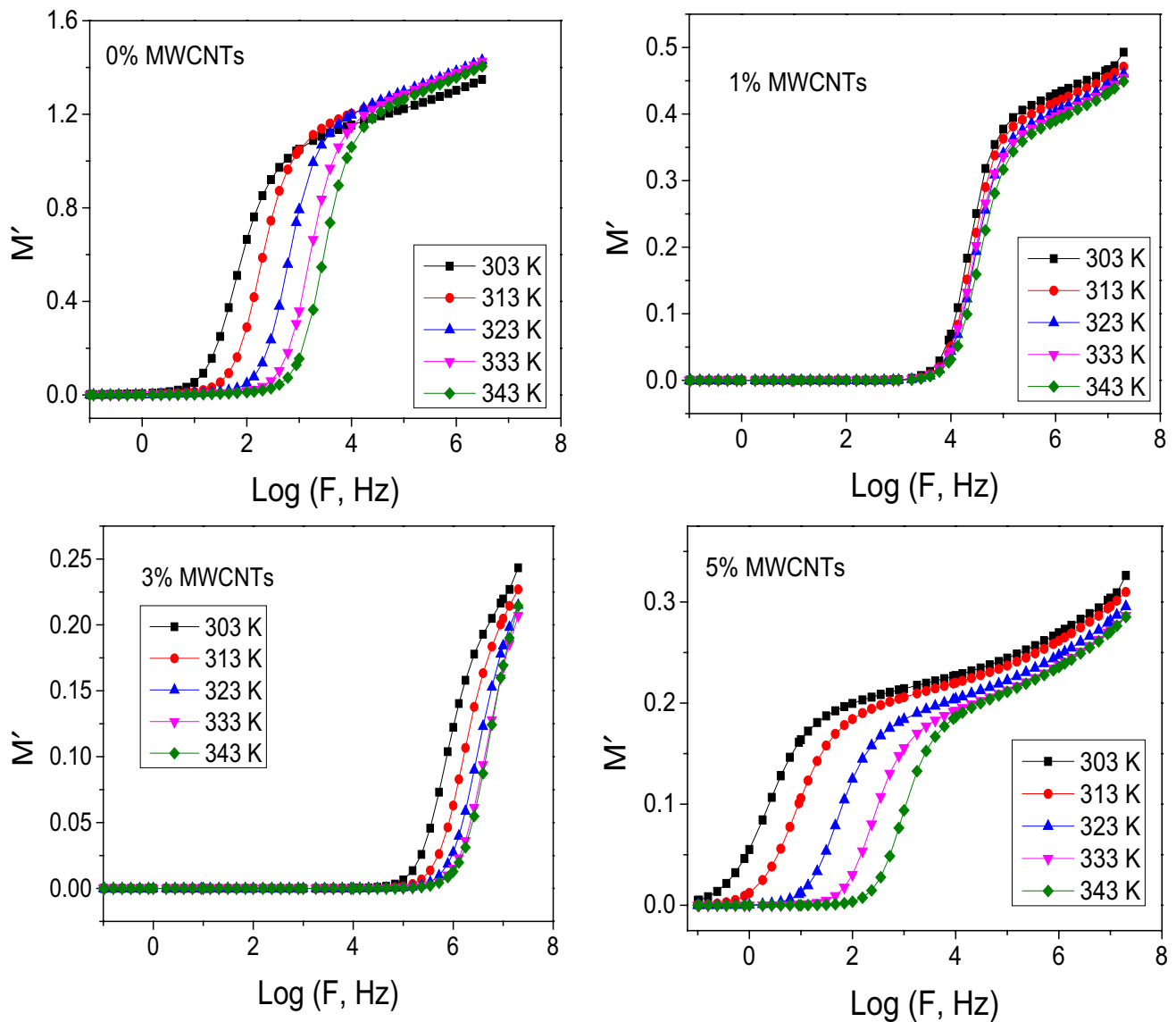


Fig. 11 The change of real part M' of the electric modulus as a function of $\text{Log}(F)$ for PVA/PVP blend filled with different MWCNTs content of at different temperatures

representative of a transition from long range to short range mobility with the frequency increase.

The physical nature of the appeared relaxation can be better understood by the analysis of relaxation parameters, which obtained from Arrhenius law:

$$f_{max} = f_0 \exp(-E_{relax}/K_B T) \quad (12)$$

where f_{max} is the peak frequency at maximum M'' , f_0 is the pre-exponential factor, and E_{relax} is the activation energy of relaxation.

Figure 13 shows the Arrhenius plots for the studied system. The activation energy E_{relax} was determined from the slope of these lines and listed in Table 4. It is found that the E_{relax} values are very close to the DC conductivity activation

energy E_{dc} . This explains that the ionic migration is responsible for the observed DC conductivity and modulus spectrum. Also, the electrical conductivity and the relaxation process are attributed to the same effect and that the charge carriers have to overcome the same energy barrier in both relaxation and conduction processes [40].

To determine whether the distribution of relaxation time is dependent on temperature or not, the M'' was displayed in scaled coordinates, i.e. M''/M''_{max} as a function of $\text{Log}(f/f_{max})$. The resultant curve is called a master electric modulus curve and used to clarify the dielectric processes taking place in the material. As shown in Fig. 14 the curves coincide on one single master curve suggesting that the relaxation time distribution is independent on temperature. This

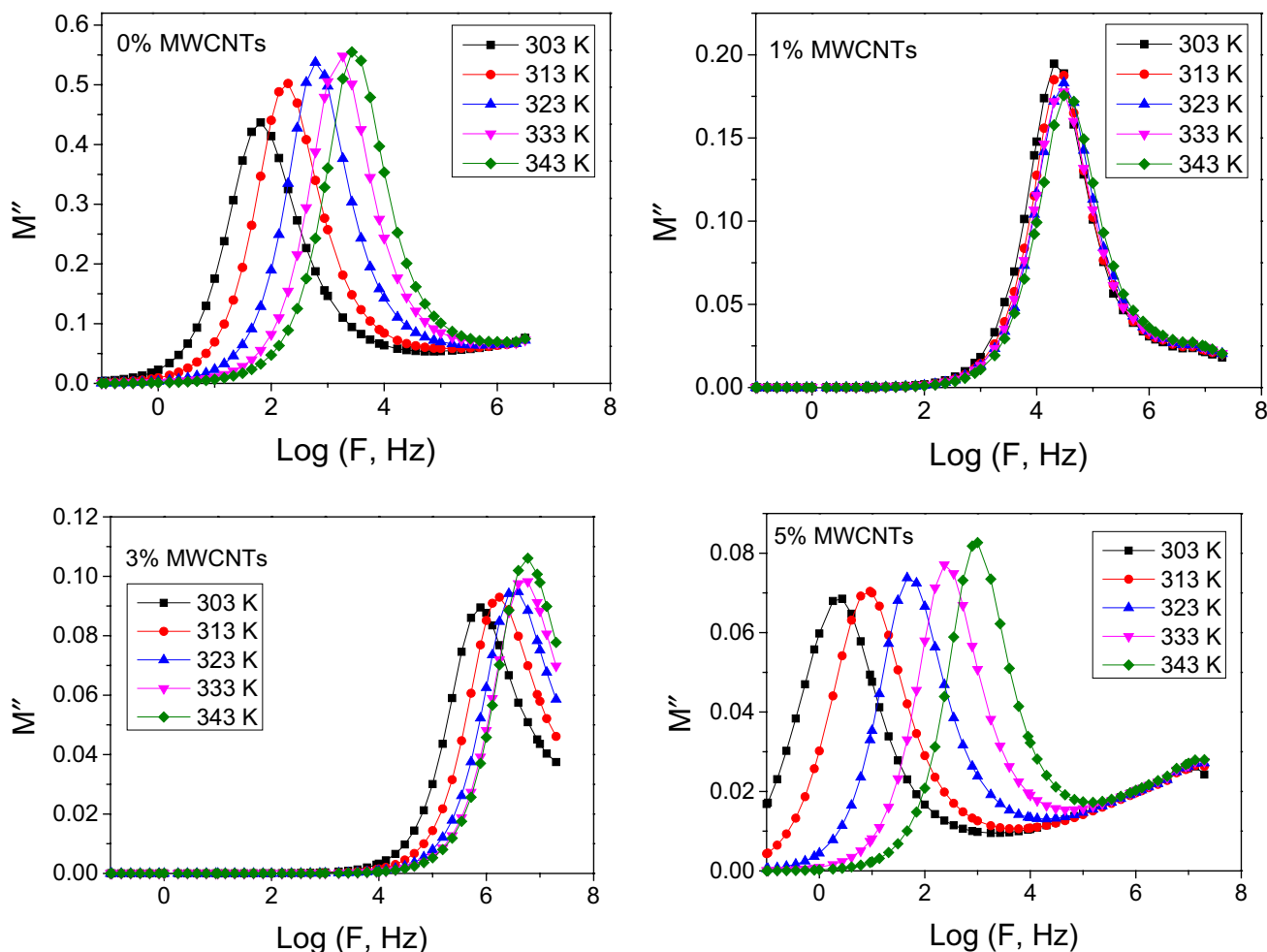


Fig. 12 The change of the imaginary part M'' of the electric modulus as a function of $\text{Log}(F)$ for PVA/PVP blend filled with different MWCNTs content at different temperatures

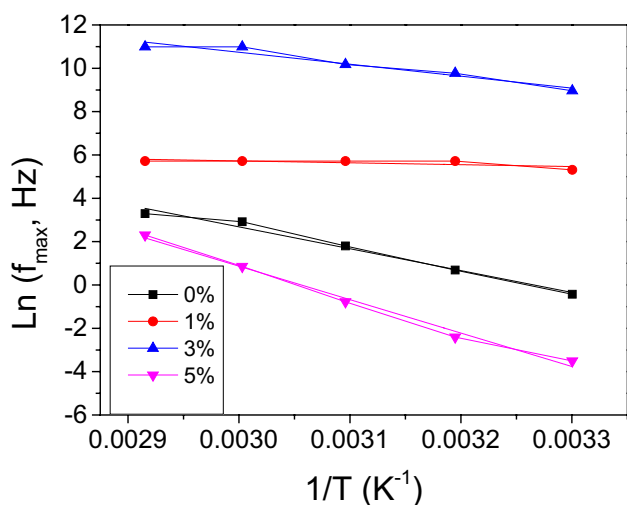


Fig. 13 Arrhenius plots for PVA/PVP blend filled with different MWCNTs content

Table 4 The activation energy E_{relax} for the present system

| MWCNTs (wt%) | E_{relax} (eV) |
|--------------|-------------------------|
| 0 | 0.86 |
| 1 | 0.07 |
| 3 | 0.47 |
| 5 | 1.32 |

implies that the conduction mechanism still unchanged and also they have the same ion transport mechanism. Therefore, the relaxation could be attributed to ions hopping motion.

The collective plot of M'' and Z'' as a function of frequency can be applied to identify whether the long or short-range movement of charge carriers is dominant in the relaxation process. The mismatch of frequency peaks between M'' and Z'' reflect that the short-range movement of charge carrier is the dominated process and deviates from the Debye-type model, whereas the frequency peaks coincidence implies that long-range movement of charge carrier

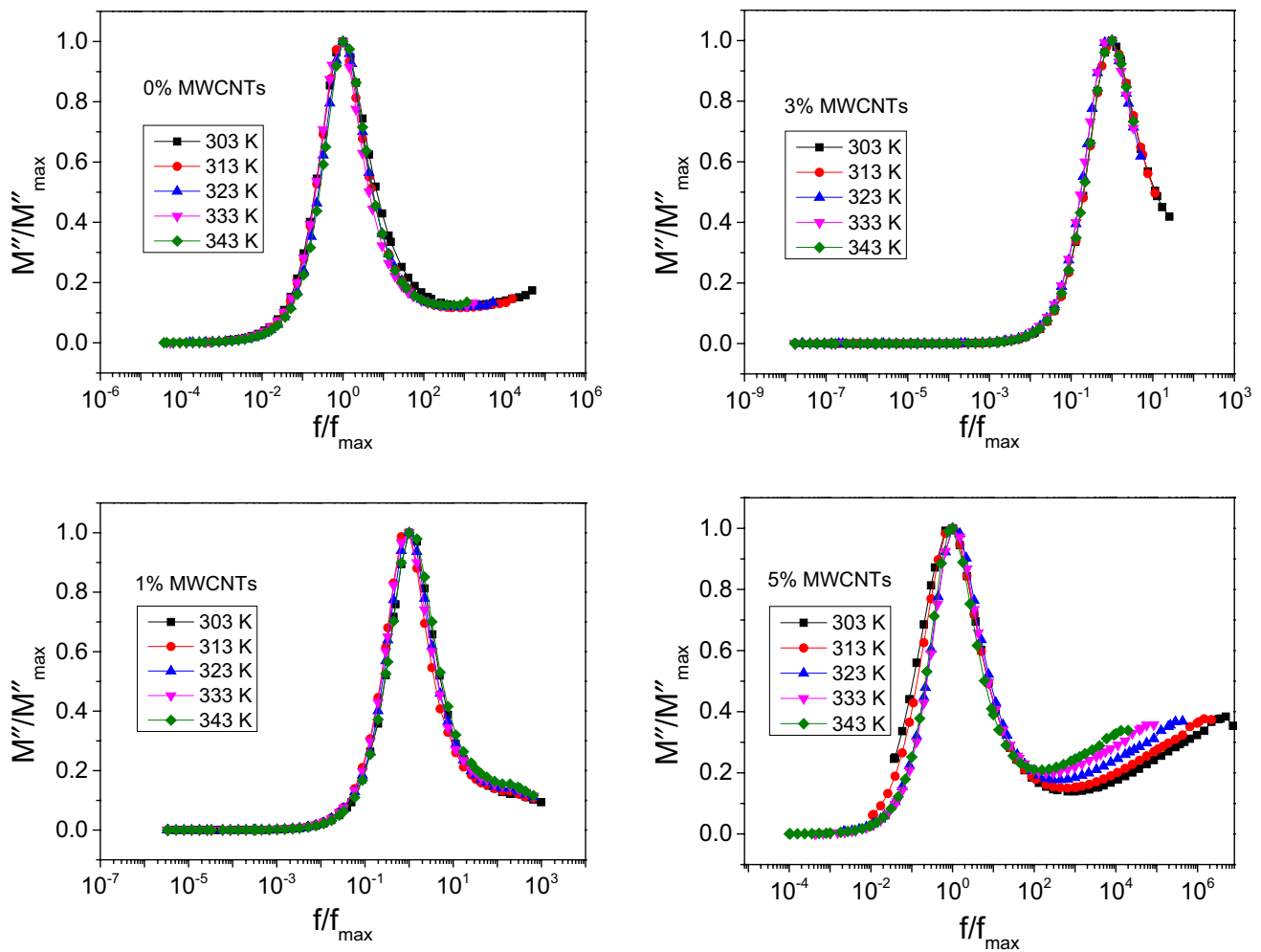


Fig. 14 The change of M''/M''_{\max} as a function of f/f_{\max} for PVA/PVP blend filled with different MWCNTs content at different temperatures

is dominant [41]. The frequency response of M''/M''_{\max} and Z''/Z''_{\max} are indicated in Fig. 15 for the sample with 3 wt% of MWCNTs at 303 and 343 K as a representative sample. From this figure, it is noticed that the M''/M''_{\max} and Z''/Z''_{\max} peaks do not coincide, indicating a non-Debye relaxation in this composite. Also, the relaxation process is because of short-range movement of charge carriers [42].

4 Conclusion

The AC electrical conductivity of PVA/PVP blend samples filled with different MWCNTs contents was studied over a wide frequency range of 10^{-1} to 10^7 Hz at different temperatures. The electrical conductivity of the composite is shown to depend on the filler type and concentration and complies with Jonscher's law. The conductivity improvement is maximum for 3 wt% of MWCNTs content, but for 5 wt% of MWCNTs, the conductivity is shown to be decreased. The

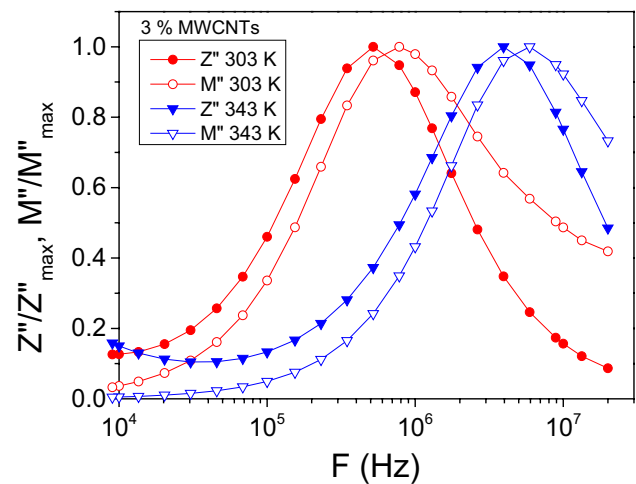


Fig. 15 The change of normalized imaginary parts of impedance Z''/Z''_{\max} and electric modulus M''/M''_{\max} as a function of frequency at temperatures 303 K and 343 K for PVA/PVP blend filled with 3 wt% of MWCNTs (as a representative sample)

temperature dependence of s-factor revealed that CBH is the suitable model for explaining carrier transport in the present samples. The experimental dielectric data were analyzed using the complex Z^* impedance formalisms and the complex M^* electric modulus. The analysis of impedance components Z' and Z'' enabled determining the samples equivalent electrical circuit. The activation energy values obtained from DC conductivity and the impedance are close and confirm that the hopping mechanism is dominated. Also, the present system obeys non-Deby relaxation and the relaxation process is due to the charge carriers short-range movement.

References

- P. Sain, R. Goyal, Y. Prasad, A. Bhargava, *J. Electron. Mater.* **46**, 458 (2017)
- G. Psarras, *Composites A* **37**, 1545 (2006)
- C.W. Nan, Y. Shen, J. Ma, *Annu. Rev. Mater. Res.* **40**, 131 (2010)
- A. Eken, E. Tozzi, D. Klingenberg, W. Bauhofer, *J. Appl. Phys.* **109**, 084342 (2011)
- W. Bauhofer, J.Z. Kovacs, *Compos. Sci. Technol.* **69**, 1486 (2009)
- Q. Zhang, H. Li, M. Poh, F. Xia, Z.Y. Cheng, H. Xu, C. Huang, *Nature* **419**, 284 (2002)
- C.V. Subba Reddy, X. Han, Q.-Y. Zhu, L.-Q. Mai, W. Chen, *Microelectron. Eng.* **83**, 281 (2006)
- H.M. Zidan, E.M. Abdelrazek, A.M. Abdelghany, A.E. Tarabiah, *J. Mater. Res. Technol.* **8**, 904 (2019)
- N. Singh, A. Qureshi, A. Rakshit, D. Avasthi, *Bull. Mater. Sci.* **29**, 605 (2006)
- M. Rahaman, A. Aldalbahi, P. Govindasami, N.P. Khanam, S. Bhandari, P. Feng, T. Altalhi, *Polymers* **9**, 527 (2017)
- A. Darwish, M. El-Nahass, A. Bekheet, *J. Alloys Compd.* **586**, 142 (2014)
- I. Austin, N.F. Mott, *Adv. Phys.* **18**, 41 (1969)
- N.F. Mott, E.A. Davis, *Electronic Processes in Non-crystalline Materials (Monographs on Physics)* (Oxford University Press, Oxford, 1979)
- K. Hemalatha, G. Sriprakash, M. Ambika Prasad, R. Damle, K. Rukmani, *J. Appl. Phys.* **118**, 154103 (2015)
- A.K. Jonscher, *Nature* **267**, 673 (1977)
- M. Sassi, A. Bettaibi, A. Oueslati, K. Khirouni, M. Gargouri, *J. Alloy. Compd.* **649**, 642 (2015)
- A. Lösche, *Cryst. Res. Technol.* **7** (1972)
- F.K. Tan, J. Hassan, Z.A. Wahab, R.S. Azis, *Eng. Sci. Technol.* **19**, 2081 (2016)
- A.K. Jonscher, *J. Phys. D* **32**, R57 (1999)
- R. Khalil, *Appl. Phys. A* **123**, 422 (2017)
- D.C. Sinclair, A.R. West, *J. Appl. Phys.* **66**, 3850 (1989)
- M. Prabu, S. Selvasekarapandian, A. Kulkarni, G. Hirankumar, A. Sakunthala, *Ionics* **16**, 317 (2010)
- O. Bohnke, S. Ronchetti, D. Mazza, *Solid State Ion.* **122**, 127 (1999)
- X. Li, S. Hsu, *J. Polym. Sci. Polym. Phys. Ed* **22**, 1331 (1984)
- C. Ramya, S. Selvasekarapandian, G. Hirankumar, T. Savitha, P. Angelo, *J. Non-Cryst. Solids* **354**, 1494 (2008)
- M. Abbassi, R. Ternane, I. Sobrados, A. Madani, M. Trabelsi-Ayadi, J. Sanz, *Ceram. Int.* **39**, 9215 (2013)
- C. Ramya, S. Selvasekarapandian, T. Savitha, G. Hirankumar, R. Baskaran, M. Bhuvanewari, P. Angelo, *Eur. Polym. J.* **42**, 2672 (2006)
- S. Lanfredi, P. Saia, R. Lebullenger, A. Hernandez, *Solid State Ion.* **146**, 329 (2002)
- A. Omri, M. Bejar, E. Dhahri, M. Es-Souni, M. Valente, M. Graça, L. Costa, *J. Alloys Compd.* **536**, 173 (2012)
- S. Selvasekarapandian, M. Vijayakumar, *Mater. Chem. Phys.* **80**, 29 (2003)
- A. James, K. Srinivas, *Mater. Res. Bull.* **34**, 1301 (1999)
- M. Ram, *Solid State Sci.* **12**, 350 (2010)
- K. Chandra, K. Prasad, R. Gupta, *Physica B* **388**, 118 (2007)
- S. Yu, P. Hing, X. Hu, *J. Appl. Phys.* **88**, 398 (2000)
- R. Gerhardt, *J. Phys. Chem. Solids* **55**, 1491 (1994)
- A. Langar, N. Sdiri, H. Elhouichet, M. Ferid, *Results Phys.* **7**, 1022 (2017)
- T. Zangina, J. Hassan, K.A. Matori, R.S. Azis, U. Ahmadu, A. See, *Results Phys.* **6**, 719 (2016)
- J. Isasi, M.L. López, M.L. Veiga, E. Ruiz-Hitzky, C. Pico, *J. Solid State Chem.* **116**, 290 (1995)
- G.E. El-Falaky, O.W. Guirguis, N.S. Abd El-Aal, *Prog. Nat. Sci.* **22**, 86 (2012)
- C. Mariappan, G. Govindaraj, S.V. Rathan, G.V. Prakash, *Mater. Sci. Eng. B* **123**, 63 (2005)
- O. Raymond, R. Font, N. Suárez-Almodovar, J. Portelles, J. Siqueiros, *J. Appl. Phys.* **97**, 084107 (2005)
- R. Tang, C. Jiang, W. Qian, J. Jian, X. Zhang, H. Wang, H. Yang, *Sci. Rep.* **5**, 13645 (2015)

Publisher's Note Springer Nature remains neutral with regard to jurisdictional claims in published maps and institutional affiliations.